Supporting Information for

Facet junction engineering for enhanced SERS activity of Ag/Cu_2O composite substrates

Ming Zhou, Xunfei He, Yinyan Gong*, Can Li, and Lengyuan Niu

Institute of Optoelectronic Materials and Devices, College of Optical and Electronic Technology, China Jiliang University, Hangzhou 310018, China

Email address: 13A0502075@cjlu.edu.cn

S1 Experimental Section

S1.1 Materials

Copric chloride dihydrate ($CuCl_2 \cdot 2H_2O$), sodium hydroxide (NaOH), ascorbic acid (AA), silver nitrate ($AgNO_3$), ethanol, 4-nitrobenzenethiol (4-NBT), rhodamine 6G (R6G), and crystal violet (CV) were purchased from aladdin (Shanghai) Co., Ltd. sodium citrate was purchased from McLean Biochemical Technology Co., Ltd. Polyvinylpyrrolidone (PVP K30) was purchased from Sinopharm Chemical Reagent Co., Ltd.

S1.2 Synthesis of Cu_2O Polyhedrons

Well-shaped Cu_2O nanocrystals of different morphology were prepared by a liquid-phase reduction method [1] with slight modification. To synthesis truncated-octahedral Cu_2O nanocrystals with co-exposed {100} and {111} facets (labeled as Cu_2O(J)), 3.33 g PVP was dissolved in aqueous solution of $CuCl_2 \cdot 2H_2O$ (100 mL, 0.01 M), followed by addition of NaOH solution (10 mL, 2 M). After 30 min, ascorbic acid solution (20 mL, 0.60 M) was added dropwisely to the obtained brownish suspension, and the mixture was aged for 60 min. The whole synthesis process was kept at 55 ℃ in water bath under magnetic stirring. The resulting products were collected, washed thoroughly by deionized water and ethanol, and dried in vacuum oven. Cube-shaped Cu_2O enclosed by {100} facets (Cu_2O(C)) and octahedron-shaped Cu_2O enclosed by {111} facets (Cu_2O(O)) were synthesized under

similar conditions except that 0 g and 4.44 g PVP were used, respectively.

SEM images in Figs. S1a-S1c confirmed successful preparation of cubic, truncated-octahedral and octahedral nanocrystals by using 0 g, 3.33 g and 4.44 g of PVP. Moreover, measured XRD patterns of all the three samples matched well with Cu_2O in cubic phase (PDF# 99-0041), and there is no diffraction signals originated from impurity phase (Fig. S1d).

S1.3 Calculation of Enhancement Factor

Enhancement factor (EF) was calculated based on the following equations [2]:

$$EF = \left(\frac{I_{SERS}}{N_{SERS}}\right) \Big/ \left(\frac{I_{NR}}{N_{NR}}\right) \quad (1)$$

$$N_{SERS} = (N_{AV} \times A_{beam})/\sigma \quad (2)$$

$$N_{NR} = C_{NR} \times V \times (\frac{A_{beam}}{A}) \times N_{AV} \quad (3)$$

where I_{SERS} and I_{NR} represent the integrated intensity of SERS and normal Raman peaks, respectively. To measure the normal Raman spectrum, 4-NBT solution (5×10^{-4} M) was drop-cast on Si wafer, and the exposure time, laser power (at sample), and accumulation were set as 30 s, 0.56 mW, and 8, respectively. N_{AV} is the Avogadro constant, σ is the surface area occupied by self-assembled monolayer of probe molecule (=3.0×10^9 cm^2/mol for 4−NBT [3]), and A_{beam} is the effective area under laser irradiation which is estimated by $A_{beam} = \pi(1.22\lambda/2NA)^2$. C_{NR} and V represent the concentration and volume of 4−NBT solution used for normal Raman spectra measurements, and A is the area formed by the solution on Si wafer. For 4-NBT, the integrated intensity of the dominant 1337 cm^{-1} peak equal to 3,756,060 (Fig.4b) and 8,124 (Fig. 4a) for SERS and normal Raman respectively. By substituting these values into equations (1-3), EF is calculated to be 5.3×10^5.

S2 Supplementary Figures

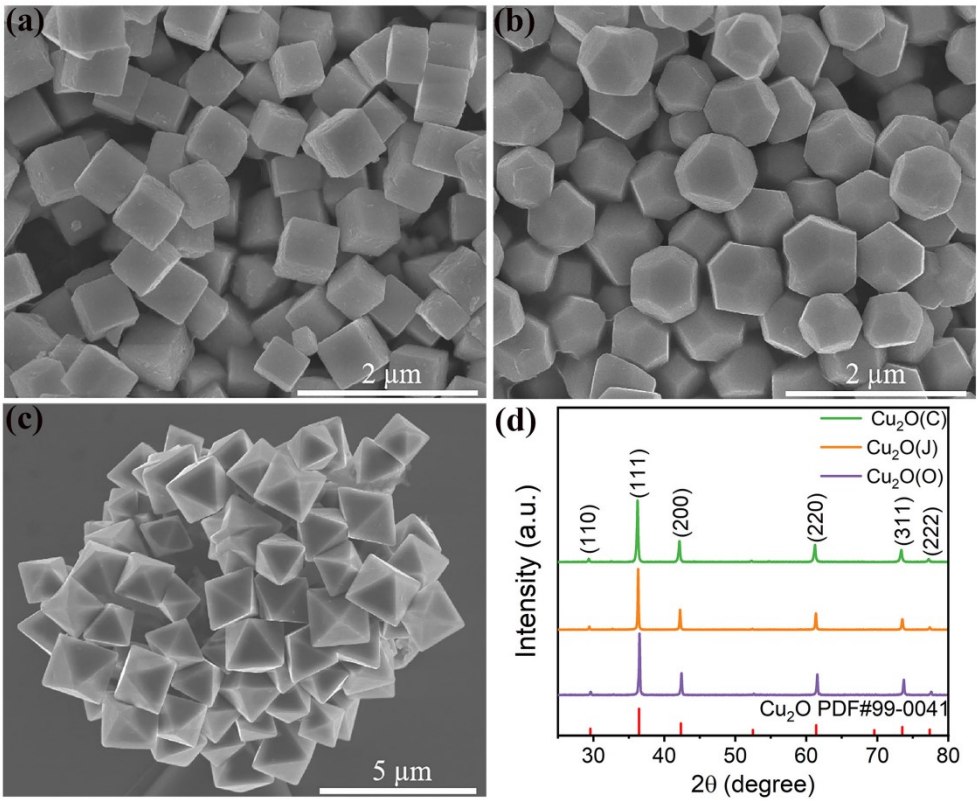

Fig. S1 (a-c) SEM images and (d) XRD curves of Cu_2O(C), Cu_2O(J) and Cu_2O(O), respectively.

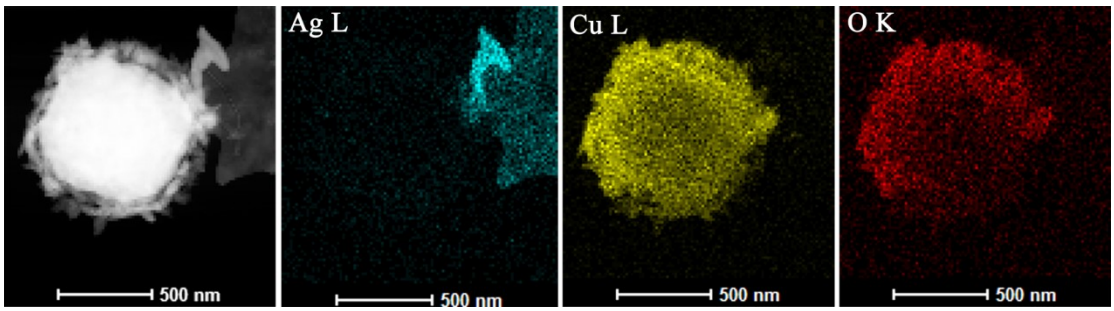

Fig. S2 Energy dispersive X-ray (EDX) elemental mapping of Ag, Cu and O in Ag/Cu_2O(J3).

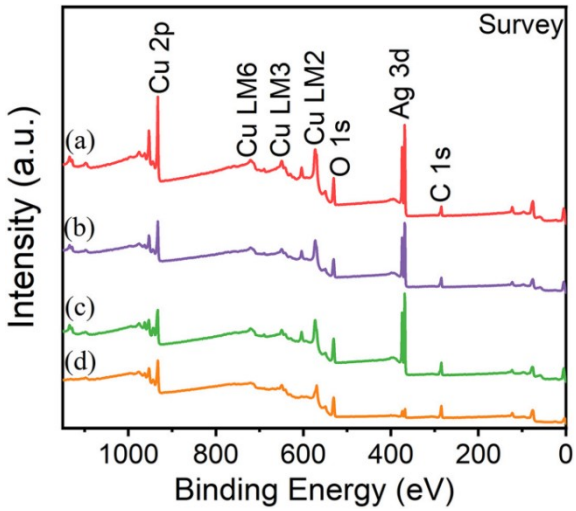

Fig. S3 XPS survey spectra of (a)Ag/Cu_2O(O), (b)Ag/Cu_2O(C), (c)Ag/Cu_2O(J3) and (d) Ag/Cu_2O(J1).

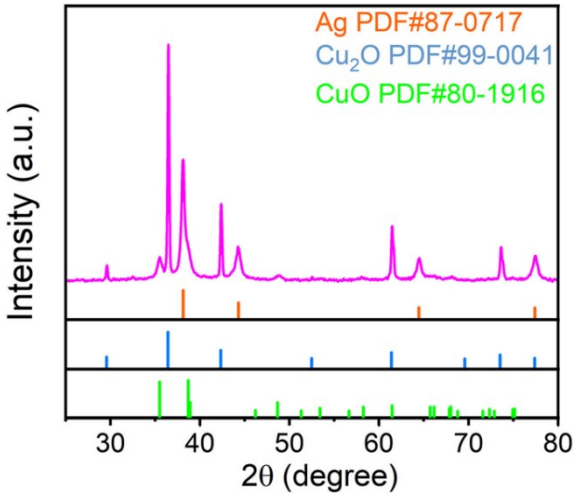

Fig. S4 XRD of Ag-decorated Cu_2O(J) prepared without the incorporation of sodium citrate.

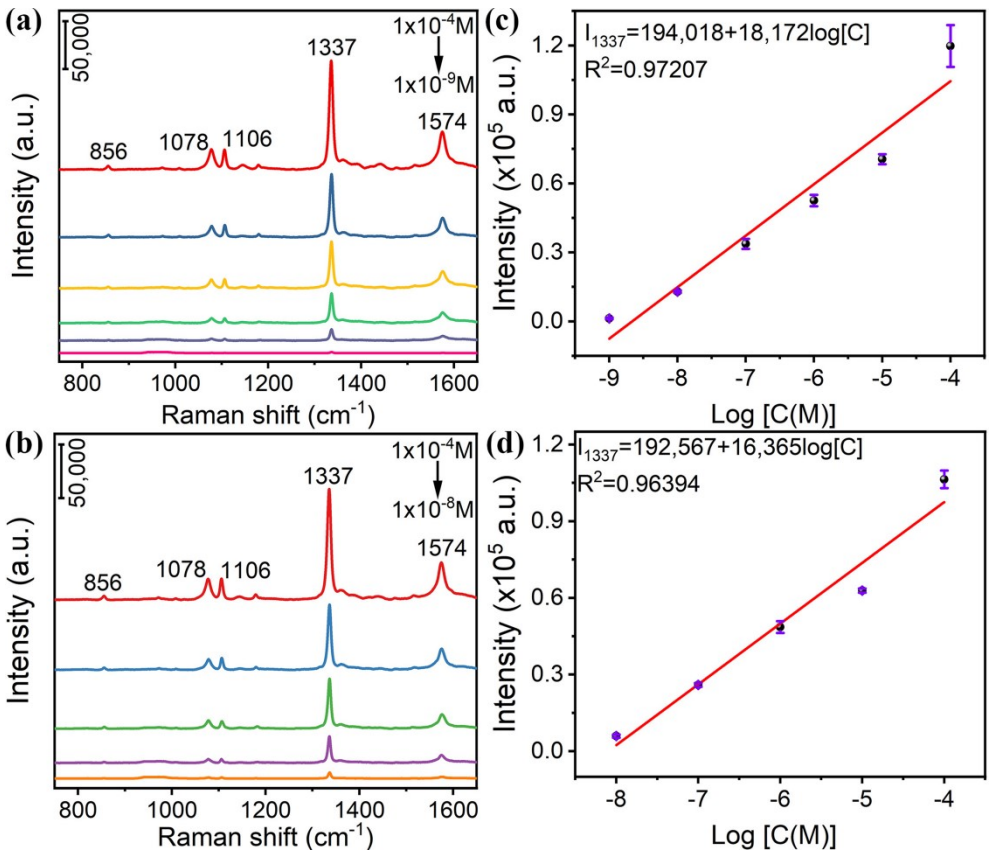

Fig. S5 (a, c) Concentration-dependent SERS spectra of 4-NBT on Ag/Cu_2O(C) and Ag/Cu_2O(O), respectively. (b, d) linear fitting of I_{1337} versus concentration for Ag/Cu_2O(C) and Ag/Cu_2O(O), respectively.

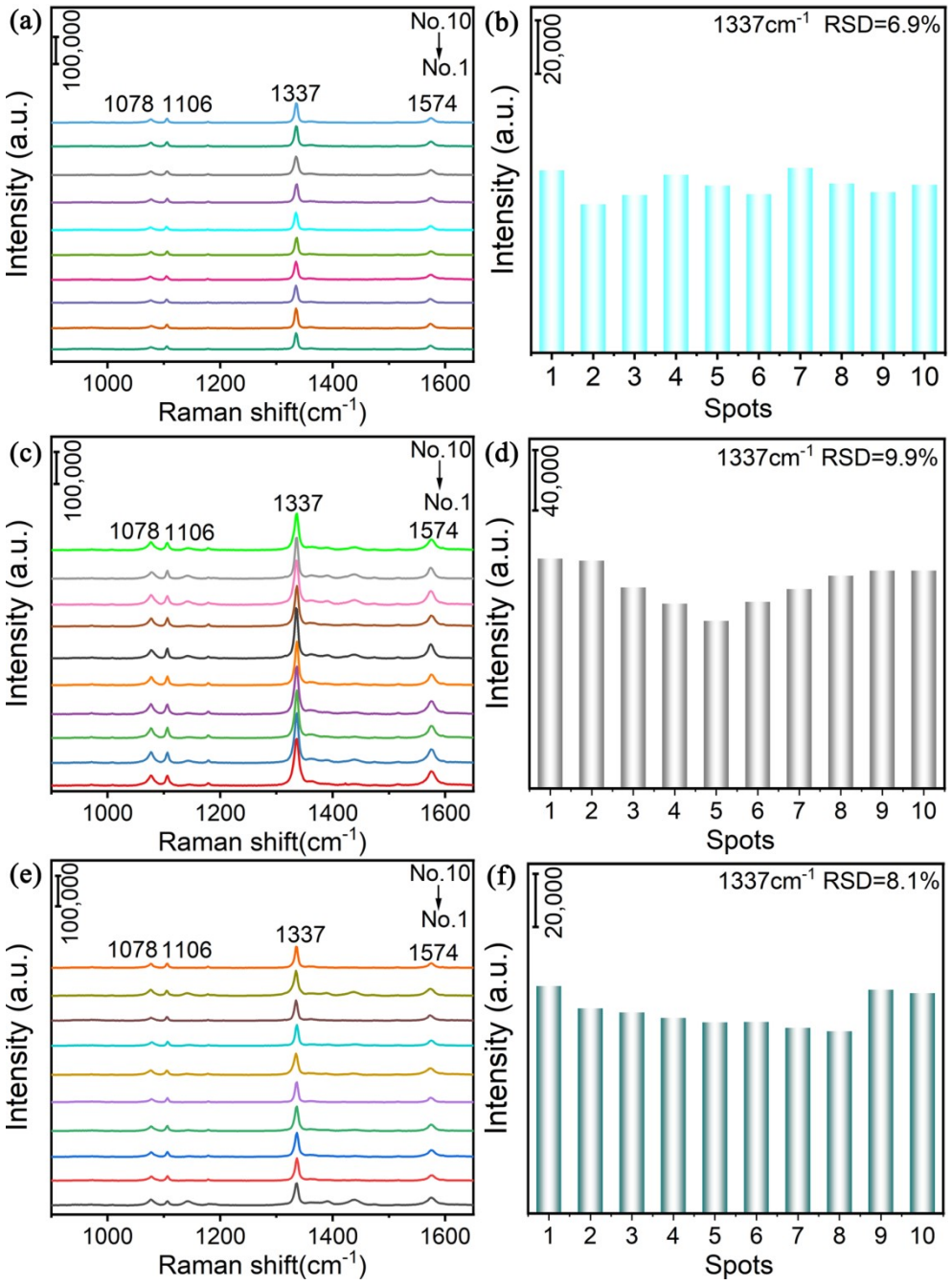

Fig. S6 SERS spectra of 1×10^{-4} M 4-NBT on (a) Ag/Cu_2O(J1), (c) Ag/Cu_2O(J2) and (e) Ag/Cu_2O(J4) acquired from ten randomly selected regions, (b, d, f) I_{1337} of different spots.

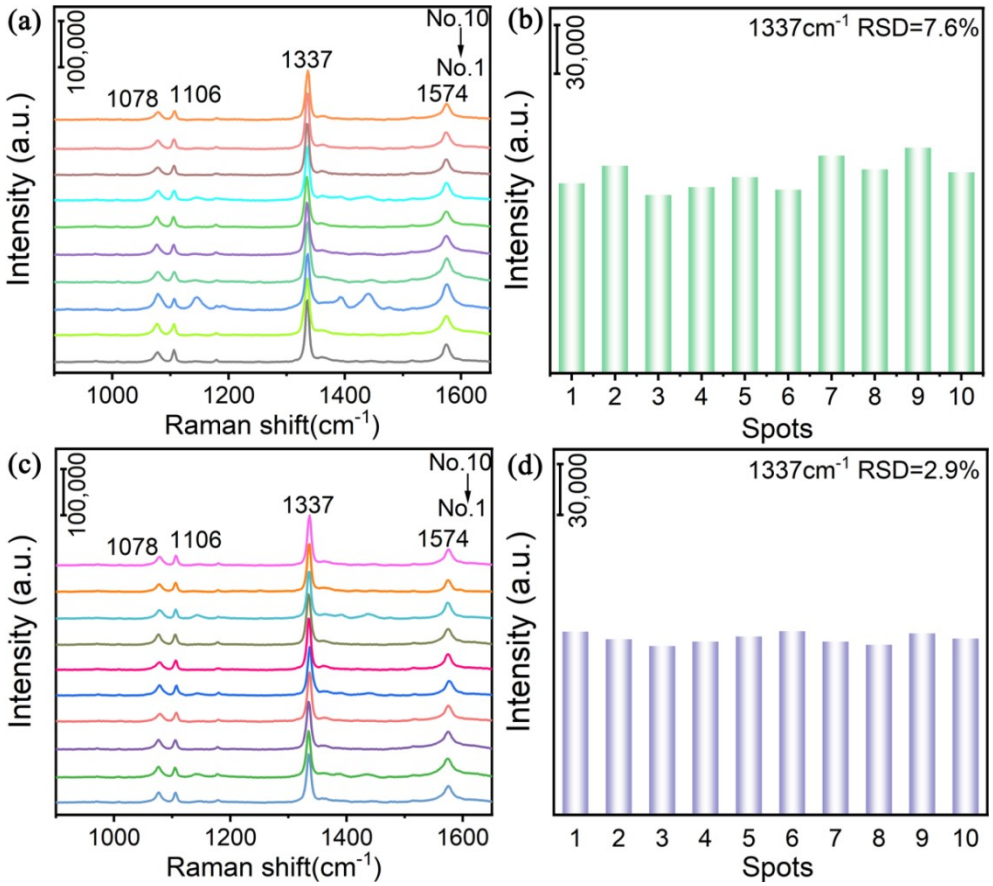

Fig. S7 SERS spectra of 1×10^{-4} M 4-NBT on (a) Ag/Cu_2O(C) and (c) Ag/Cu_2O(O) acquired from ten randomly selected regions, (b, d) I_{1337} of different spots.

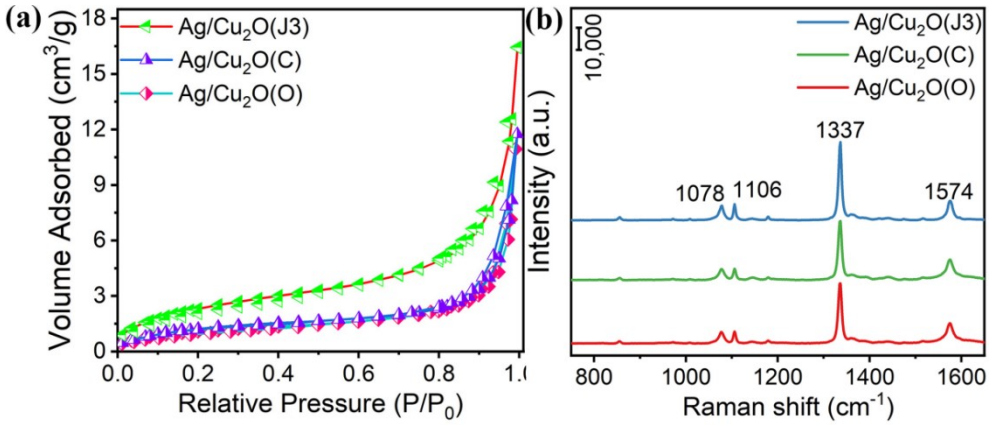

Fig. S8 (a) N_2 adsorption-desorption isotherms (b) normalized SERS spectra of Ag/Cu_2O(C), Ag/Cu_2O(J3) and Ag/Cu_2O(O).

S3 Supplementary Tables

Table S1 Synthesis conditions of Ag-decorated Cu_2O nanocrystals

Sample	PVP (g)	Cu_2O nanocrystal	$AgNO_3$ (mmol)
Cu_2O(C)	0	/	/
Cu_2O(J)	3.33	/	/
Cu_2O(O)	4.44	/	/
Ag/Cu_2O(J1)	/	Truncated-octahedrons	0.02
Ag/Cu_2O(J2)	/	Truncated-octahedrons	0.04
Ag/Cu_2O(J3)	/	Truncated-octahedrons	0.08
Ag/Cu_2O(J4)	/	Truncated-octahedrons	0.12
Ag/Cu_2O(C)	/	cubes	0.08
Ag/Cu_2O(O)	/	octahedrons	0.08

Table. S2. Comparison of sensitivity and detection limit with several substrates in literature.

Material	Analytes	EF	LOD (M)	Excitation (nm)	Reference
Au/H-g-C_3N_4	CV	6.8×10^5	2.7×10^{-9}	785	4
TiO_2-Ag-GO	CV	7.8×10^5	1×10^{-10}	785	5
Au@TiO_2 NRAs	R6G	10^4	1×10^{-7}	785	6
SiO2@Au NPs	R6G	1.5×10^6	1×10^{-8}	633	7
Flower-like MoS_2@Ag	4−MBA	1.1×10^6	1×10^{-10}	532	8
$Ti_3C_2T_x$/Ag	4−NBT	4.2×10^5	1×10^{-11}	532	9
Fe_3O_4@COF@Ag	Ciprofloxacin	/	1×10^{-9}	/	10
Fe_3O_4@PEI-DTC-Ag	thiram		1×10^{-9}		11
Ag/Cu_2O(J3)	4−NBT	5.3×10^5	1×10^{-11}	532	**This work**

References

[1] D.-F. Zhang, H. Zhang, L. Guo, K. Zheng, X.-D. Han, Z. Zhang, J. Mater. Chem., 2009, **19**, 5220-5225.

[2] X. Wang, W. Shi, Z. Jin, W. Huang, J. Lin, G. Ma, S. Li, L. Guo, Angew. Chem. Int. Edit., 2017, **56**, 9851-9855.

[3] J. Huang, Y. Zhu, M. Lin, Q. Wang, L. Zhao, Y. Yang, K.X. Yao, Y. Han, J. Am. Chem. Soc., 2013, **135**, 8552-8561.

[4] W. Tang, Y. An, K.H. Row, Chem. Eng. J., 2020, **402**, 126194.

[5] M. Zhang, T. Chen, Y. Liu, J. Zhang, H. Sun, J. Yang, J. Zhu, J. Liu, and Y. Wu, ACS Sensors, 2018, **3**, 2446-2454

[6] Z. Xie, F. Zhao, S. Zou, F. Zhu, W. Wang, Z. Zhang, J. Alloy. Compd., 2021, **861**, 157999.

[7] D. Song, T. Wang, L. Zhuang, Nanomaterials, 2023, **13** 2156.

[8] Y. Chen, H. Liu, Y. Tian, Y. Du, Y. Ma, S. Zeng, C. Gu, T. Jiang, and J. Zhou, ACS Appl. Mater. Interfaces, 2020, **12** 14386−14399.

[9] X. Xue, L. Chen, C. Zhao, M. Lu, Y. Qiao, J. Wang, J. Shi, L. Chang, Spectrochim. Acta. A, 2023, **302**, 123019.

[10] Z. Yang, G. Chen, C. Ma, J. Gu, C. Zhu, L. Li, H. Gao, Talanta, 2023, **263** 124725.

[11] K. Liu, W. Feng, Y. Li, D. Han, T. Wu, K. Li, S. Yang, J Photoch. Photobio. A-Chem., 2024, **454**, 115696.